fire

MDPI

Article

Research on Spontaneous-Combustion Prevention and Control Technology in Gob-Side Entry Retaining Goaf

Jiuling Zhang [1,2,*], Jinghan Zhang [1,2], Ying Liu [1,2], Jiuyuan Fan [1,2], Huiyong Niu [3] and Ruijiang Zhang [4]

[1] School of Emergency Management and Safety Engineering, North China University of Science and Technology, Tangshan 063210, China
[2] Key Laboratory of Mining Development and Safety Technology, Tangshan 063210, China
[3] School of Civil and Resource Engineering, University of Science and Technology Beijing, Beijing 100083, China
[4] Kailuan (Group) Co., Ltd., Tangshan 063000, China
* Correspondence: zhangjiuling@ncst.edu.cn; Tel.: +86-15100529991

Abstract

Severe air leakage in the goaf of gob-side entry retaining panels can intensify oxygen supply to residual coal and consequently increase the probability of coal spontaneous combustion. Taking the 3451S working face of a coal mine in Hebei Province as the engineering case, this study integrated in situ beam-tube monitoring with Fluent-based numerical simulation to characterize the evolution of the spontaneous-combustion three zones and to optimize prevention and control measures. The results demonstrate that the oxidation zone is characterized by an inclined, continuous band-like distribution penetrating the goaf. The simulated oxygen distribution is consistent with the field measurements, demonstrating the reliability of the established numerical model. The ventilation pattern markedly affects the air-leakage flow field and oxygen concentration distribution, and the Y-type ventilation mode exhibits a higher spontaneous-combustion risk. When the air-volume ratio between the 3451S haulage roadway and the gob-side retained entry is adjusted to 3:1, the oxidation-zone area decreases by approximately 11%. A combined control strategy involving cement-blanket and polymer-spraying leakage sealing, together with precise nitrogen injection, is then proposed to improve the goaf oxygen environment. At a nitrogen-injection rate of 600 m^3/h, the oxidation-zone area is reduced by 11,160 m^2 and the CO concentration remains stable at approximately 4.9 ppm, providing field evidence for improved fire-prevention performance. These results support the design of targeted spontaneous-combustion control strategies for gob-side entry retaining goafs.

Keywords: spontaneous-combustion "three zones"; gob-side entry retaining; beam-tube monitoring; fluent numerical simulation; precise nitrogen injection

Check for updates

Academic Editors: Baolin Qu, Jingxin Wang, Xiyang Fang and Lintao Hu

Received: 20 May 2026
Revised: 25 June 2026
Accepted: 29 June 2026
Published: 6 July 2026

Copyright: © 2026 by the authors. Licensee MDPI, Basel, Switzerland. This article is an open access article distributed under the terms and conditions of the Creative Commons Attribution (CC BY) license.

1. Introduction

Coal mining operations are exposed to multiple natural hazards, among which mine fire remains one of the most serious threats to underground safety [1]. Approximately 85% to 90% of mine fires originate from coal spontaneous combustion [2,3]. Such events not only consume coal resources but may also induce secondary coal-dust or gas combustion and explosion accidents, thereby threatening underground personnel [4–6]. Gob-side entry retaining can enhance coal recovery, reduce the excavation-to-mining ratio, and ease roadway development pressure [7–9]. However, because the retained entry is directly connected with the caving zone of the goaf, both frictional and local resistances along

air-leakage pathways are reduced. This connection enlarges the leakage-affected region, modifies the spatial distribution of spontaneous-combustion hazard zones, and increases the likelihood of residual-coal oxidation [10,11]. To control the additional spontaneous-combustion risk induced by intense air leakage near a gob-side retained entry [12], it is essential to identify the spontaneous-combustion three zones accurately and to design site-specific air-leakage sealing and inerting measures [13–15].

Under pillarless mining with gob-side entry retaining, Y-type and W-type ventilation layouts are commonly used. Hu et al. examined the evolution of residual-coal spontaneous combustion in a gob-side entry retaining goaf through confined oxygen consumption experiments. In particular, numerical simulation has become an important tool for analyzing air-leakage flow fields, oxygen migration, and the spatial development of spontaneous-combustion hazardous zones. Recent CFD-based studies have shown that computational fluid dynamics can effectively support the analysis of airflow evolution, gas transport, thermal–gas–solid coupling, and inert-gas injection strategies in longwall goaf environments. CFD simulations have also been applied to underground mine fire and ventilation problems, demonstrating their applicability for capturing turbulent eddies, smoke dispersion, and complex airflow structures under confined underground conditions. Zhang et al. [16] quantified air leakage and the spatial distribution of hazardous zones by combining field tests with numerical simulations. Zhou et al. [17] developed a laboratory platform to investigate air-leakage behavior adjacent to a retained entry. Zhou et al. [18] analyzed how nitrogen-injection parameters affect the oxidation zone using numerical modeling. Jing et al. [19] addressed the intensified residual-coal oxidation risk caused by roof-cutting and pressure-relief mining, and optimized nitrogen-injection parameters through a Behnken response-surface design. Zhang et al. [20] proposed an integrated fire-control system combining leakage sealing with goaf nitrogen injection based on numerical analysis. Luo et al. [21] characterized goaf air-leakage fields through field measurement and statistical analysis, and verified control measures involving ventilation-duct optimization, pressure adjustment, and composite-material spraying.

Although previous studies have provided valuable insights into air-leakage characteristics, spontaneous-combustion zone evolution, and nitrogen-injection control in gob-side entry retaining goafs, several issues remain insufficiently addressed. First, most existing studies focus on a single ventilation layout or an individual control measure, while comparative analyses of Y-type and W-type ventilation under consistent geometric and boundary conditions remain limited. Second, the coupling relationship among air-leakage flow, oxygen concentration distribution, and the spatial evolution of the spontaneous-combustion three zones has not been fully clarified using both field monitoring and numerical validation. Third, existing prevention strategies often consider leakage sealing or nitrogen injection separately, whereas quantitative optimization of integrated measures involving ventilation regulation, air-leakage sealing, and precise nitrogen injection is still inadequate. These limitations restrict the development of site-specific prevention and control strategies for spontaneous combustion in gob-side entry retaining goafs. Using the goaf of the 3451S working face in a Hebei coal mine as the engineering prototype, this work compares the air-leakage flow field, oxygen concentration field, and spontaneous-combustion three-zone distribution under Y-type and W-type ventilation through Fluent numerical simulation. On this basis, optimized prevention and extinguishing measures are developed to support the safe application of gob-side entry retaining technology in underground coal mining.

2. Field Measurement of Spontaneous-Combustion Three Zones in the Gobs

2.1. Working Face Overview

The studied mine has a designed production capacity of 4.5 Mt/a, proven geological reserves of 177.60 Mt, and a minefield area of 32.33 km^2. The absolute and relative gas emission rates are 390.6 m^3/min and 24.07 m^3/t, respectively. The 3451S working face extracts a coal seam with Class II spontaneous-combustion tendency. The seam is nearly horizontal, with a thickness of 0.1–2.4 m, a strike length of 1067 m, and a dip length of 185.1 m.

2.2. Coal Sample Characterization and Programmed-Temperature Oxidation Experiment

2.2.1. Coal Sample Preparation and Proximate Analysis

The collected coal blocks were crushed and sieved into 100–200-mesh and 60–80-mesh fractions. Experiments were conducted using a 5E-MAG6700 automatic industrial analyzer (Changsha Kaiyuan Instruments Co., Ltd., Changsha, China). Proximate analysis showed that the moisture, ash, volatile matter, and fixed carbon contents were 3.59%, 28.10%, 28.65%, and 40.66%, respectively. Ultimate analysis indicated that the C, H, O, and N contents were 63.59%, 4.15%, 14.22%, and 0.97%, respectively.

2.2.2. Programmed-Temperature Oxidation Experiment

The oxygen consumption rate was determined using a model GC-4085B automatic gas chromatograph dedicated for coal mines (EWAI, Beijing, China). A 60 g coal sample with a particle size of 60–80 mesh was loaded into the sample chamber. The airflow rate was maintained at 100 mL min^{-1}, and the temperature was increased from 30 to 240 °C at a heating rate of 0.5 °C min^{-1}. During the test, gas samples were collected at 10 °C intervals, and the gas composition and concentration were determined by gas chromatography.

2.2.3. Oxygen Consumption Rate and Heat Release Intensity

The oxygen consumption rate, as an indicator of the oxidation degree of coal samples, can indirectly reflect their propensity for spontaneous combustion [22,23].

$$v(T) = \frac{QC_1}{SL} ln \frac{C_1}{C_2} \quad (1)$$

where

$v(T)$—Oxygen consumption rate of coal samples, mol/(cm^3·s).
T—Temperature, K.
S—Cross-sectional air supply area of the coal sample chamber, cm^2.
Q—Airflow rate, L/min.
C_1—Inlet oxygen concentration of the coal sample chamber, mol/m^3.
C_2—Outlet oxygen concentration of the coal sample chamber, mol/m^3.
L—Distance traveled by oxygen through the coal sample chamber, cm.

The oxygen consumption rate increased slowly during the initial oxidation stage but rose markedly once the temperature exceeded 120 °C. As shown in Figure 1, the oxygen consumption rate increased with increasing coal temperature.

2.3. Field Measurement Scheme

A pre-embedded beam-tube monitoring scheme was used to determine the oxygen concentration in the goaf and to delineate the spontaneous-combustion three zones. The monitoring points were installed at the upper corner on the return-air side of the working face. Protective casings were arranged to prevent tube damage, and three-way connectors

were used to protect the sampling heads. The casings were fixed to the roadway surface using gangue pads, and the sampling points were maintained 1.5 m above the floor. As the working face advanced, the beam tubes were progressively buried in the goaf, allowing daily gas analysis to track the oxidation state of residual coal. The working face adopted Y-type ventilation, and the beam-tube layout is illustrated in Figure 2.

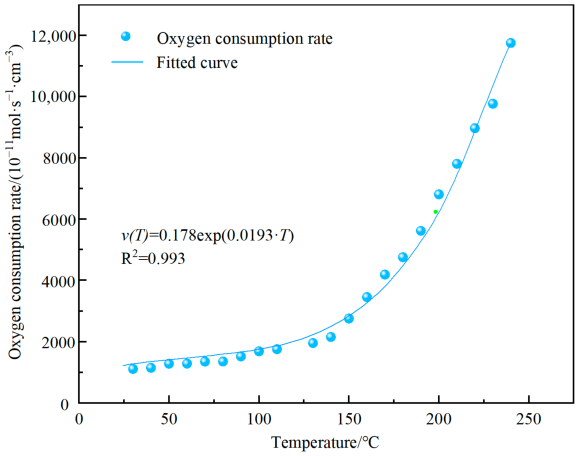


Figure 1. Oxygen consumption rate curve.

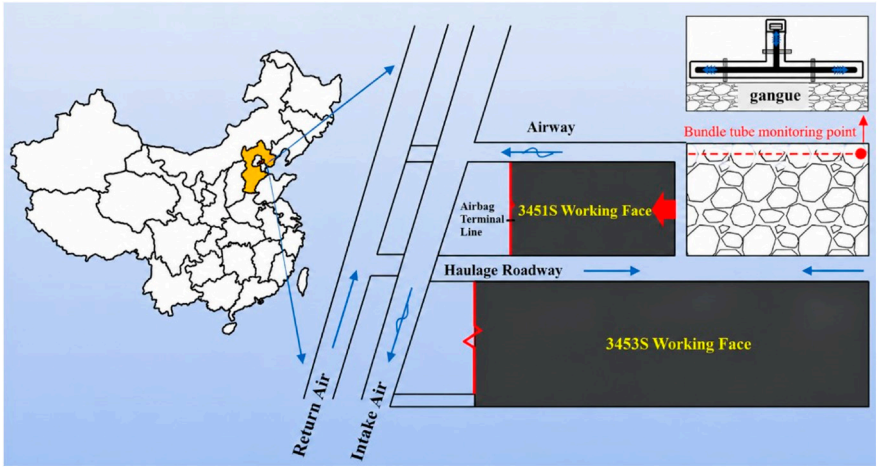


Figure 2. Layout of beam tubes for 3451S working face. Blue arrows indicate airflow direction, red arrows indicate the working-face advance direction, and red dot denote the bundle-tube monitoring line and monitoring point.

2.4. Measurement Results

According to commonly used goaf fire-prevention practice and previous studies on coal spontaneous combustion, the area with an O_2 concentration higher than 18% was classified as the heat-dissipation zone, where sufficient air leakage exists but heat is readily removed by airflow. The region with an O_2 concentration between 5% and 18% was defined as the oxidation zone, in which residual coal can continuously consume oxygen and accumulate heat. When the O_2 concentration decreased below 5%, the area was regarded as the suffocation zone, where the oxygen-deficient environment significantly inhibits residual-coal oxidation. Therefore, the 18% and 5% O_2 concentration contours were used as the upper and lower boundaries of the oxidation zone, respectively.

Based on the gas data obtained from the buried beam tubes, the variation in O_2 concentration at monitoring depths of 19–75 m in the goaf was plotted using Origin, as presented in Figure 3.

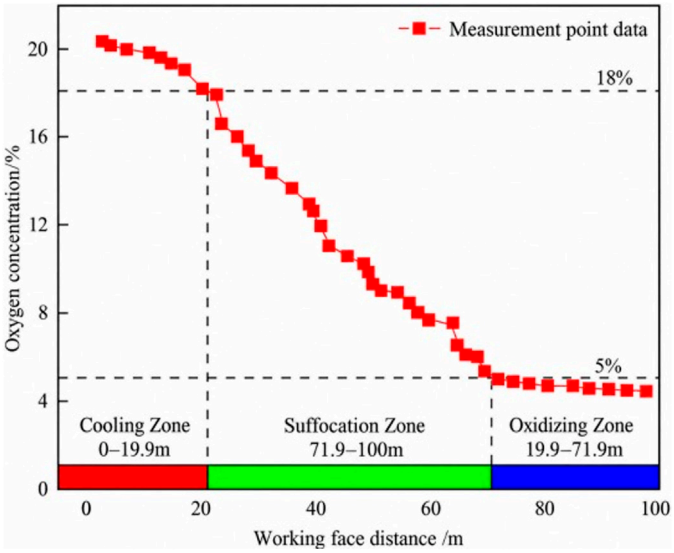


Figure 3. Variation curve of O_2 concentration at monitoring points.

As shown in Figure 3, the monitoring points moved progressively deeper into the goaf with face advance, while the O_2 concentration exhibited a continuous decreasing tendency. At 19.9 m from the working face, the O_2 concentration decreased to 18.21%, indicating entry into the oxidation zone. When the distance increased to 71.9 m, the O_2 concentration further declined to 4.97%, corresponding to the suffocation zone. This attenuation is mainly attributed to continuous oxygen consumption by residual-coal oxidation and the limited replenishment of fresh air through leakage pathways. According to the monitoring results, the spontaneous-combustion zones on the return-airway side of the 3451S goaf are divided as follows: heat-dissipation zone, 0–20 m; oxidation zone, 20–71 m.

3. Physical Model Construction of Gob with Gob-Side Entry Retaining

3.1. Basic Assumptions of the Model

Considering the complexity of the underground goaf environment, the following simplifications were introduced to establish a tractable model for analyzing spontaneous-combustion hazards.

- The goaf was treated as a heterogeneous porous medium.
- The effects of roadway equipment and pipelines on the simulated flow field were not considered.
- Moisture evaporation and gas desorption from coal were excluded from the coal spontaneous-combustion model.
- The inlet airflow was assumed to contain no gas, and gas emission from the coal wall was ignored.

3.2. Geometric Model

During coal extraction, the ventilation layout plays a controlling role in the spatial development of the air-leakage flow field and oxygen concentration field within the goaf. Therefore, the present numerical model was designed to compare the influence of different ventilation configurations. Considering the use of gob-side entry retaining, two representative ventilation schemes were selected:

- Y-type ventilation: fresh air enters through the 3451S haulage roadway and the gob-side retained entry, and the 3451S return roadway serves as the return-air outlet.
- W-type ventilation: the 3451S and 3453S haulage roadways act as intake airways, whereas the 3451S return roadway is used for airflow discharge.

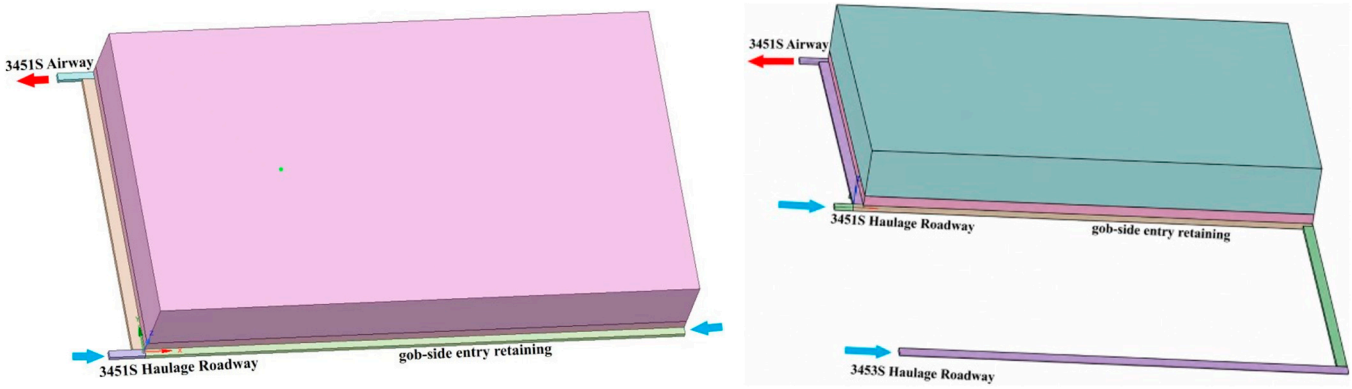
- The goaf models established for the two ventilation layouts are shown in Figure 4, and their geometric parameters are summarized in Tables 1 and 2.

Table 1. Model parameters of the gob (Y-type ventilation).

Item	Parameters/(Length × Width × Height)
Gob	300 m × 167 m × 35 m
Working Face	167 m × 6.7 m × 2.6 m
Gob-Side Entry Retaining	300 m × 4 m × 2.6 m
3451S Haulage Roadway, 3451S Air Return Roadway	20 m × 4 m × 2.6 m

Table 2. Model parameters of the gob (W-type ventilation).

Item	Parameters/(Length × Width × Height)
Gob	300 m × 167 m × 35 m
Working Face	167 m × 6.7 m × 2.6 m
Gob-Side Entry Retaining	300 m × 4 m × 2.6 m
3451S Haulage Roadway	20 m × 4 m × 2.6 m
3451S Air Return Roadway	320 m × 4 m × 2.6 m
3453S Haulage Roadway	



(**a**) Y-type ventilation (**b**) W-type ventilation

Figure 4. Physical model of the gob. Blue arrows indicate intake airflow directions, and red arrows indicate return airflow through the 3451S airway. Different colors are used to distinguish the main model components, including the goaf, haulage roadways, and gob-side entry retaining section.

3.3. Boundary Conditions

The boundary conditions adopted in the goaf numerical model are summarized in Table 3.

Table 3. Boundary conditions of gob in gob-side entry retaining.

Item	Parameter
Wind speed in 3451S haulage roadways and gob-side entry retaining	1.2 m/s
Gravity/(N·kg^{-1})	−9.81
Turbulence Model	RNG *k*-ε Model
Species	Methane-air
Airflow inlet type	Velocity inlet
Airflow outlet type	Outlet
Energy convergence	10^{-6}
Air duct velocity	10 m/s

The RNG k–ε turbulence model was selected because it improves the treatment of rapidly strained and swirling flows compared with the standard k–ε model, making it suitable for simulating air leakage in the roadway–goaf system. In particular, the model can reasonably capture flow separation, turbulent mixing, and vortex structures near the gob-side retained entry and cut-hole region, while maintaining computational stability for full-scale engineering simulations.

3.4. Simulation Verification

The numerical model was validated by comparing the simulated oxygen concentration with the field data obtained from beam-tube monitoring. This comparison was used to assess the reliability of subsequent simulations under different ventilation conditions. The oxygen concentration distribution under Y-type ventilation is displayed in Figure 5, and the measurement–simulation comparison is provided in Figure 6.

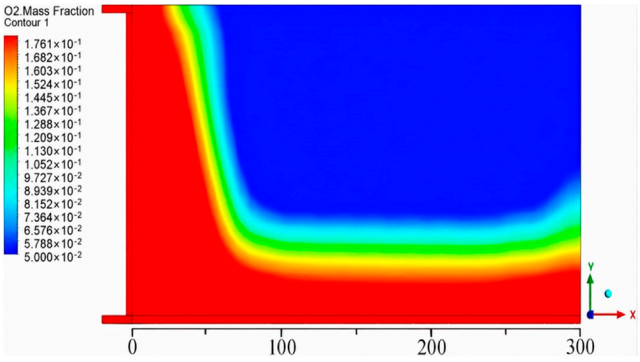


Figure 5. Spatial distribution of oxygen concentration in the goaf.

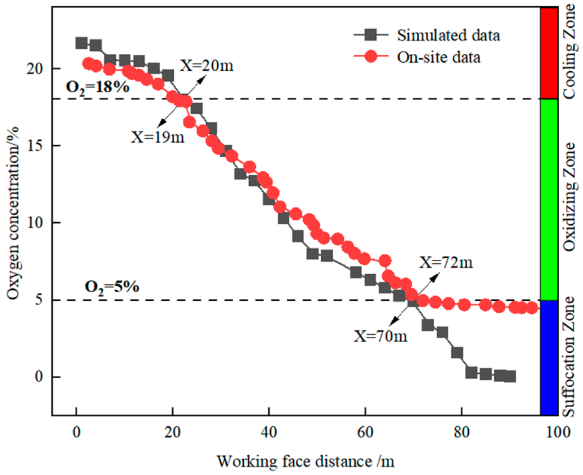


Figure 6. Comparison of measured points and simulation results.

Figure 5 indicates that the goaf oxidation zone forms an inclined penetrating band. On the return-airway side, the 18% and 5% oxygen concentration contours are located approximately 19 m and 70 m from the working face, respectively. At the tail of the retained-entry section, the corresponding contours occur at distances of 35 m and 91 m from the gob-side retained entry. Thus, the oxidation zone near the retained-entry tail is wider and extends farther into the goaf than that in the middle part of the working face. This pattern is associated with the relatively high pressure at the tail, which promotes air leakage into the goaf.

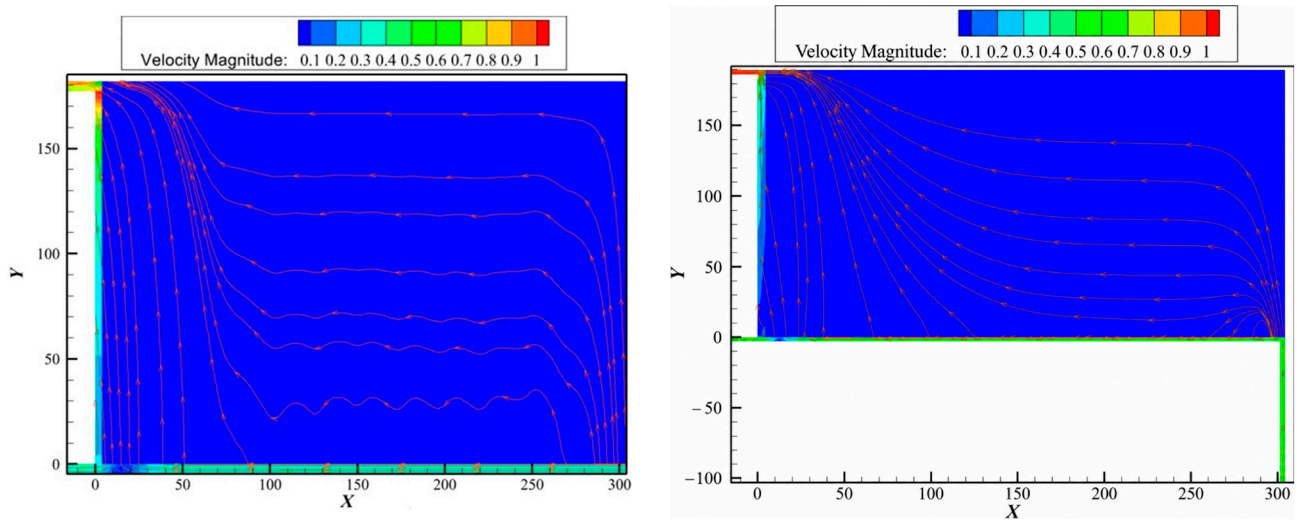
As shown in Figure 6, the oxidation-zone width measured by beam-tube monitoring on the return-airway side is 52 m, whereas the simulated value is 51 m. The small deviation

between the two results, together with the similar O_2 concentration trends, confirms the rationality and accuracy of the numerical model. Therefore, the model can be used for subsequent identification of spontaneous-combustion hazardous zones and for optimization of fire-prevention measures in the goaf.

4. Air-Leakage Flow Field and Oxygen Distribution in the Gob Under Different Ventilation Configurations

4.1. Distribution Characteristics of Air-Leakage Flow Field in Gob

Figure 7a,b show that the overall air-leakage flow patterns in the goaf are comparable under the two ventilation layouts. Near the working face, two air streams converge in the gob-side retained entry and generate a turbulent region with a large-scale vortex. Under centrifugal effects, this region further develops into a deceleration and pressurization zone, where vortical flow is formed.



(**a**) Velocity streamline distribution under Y-type ventilation (**b**) Velocity streamline distribution under W-type ventilation.

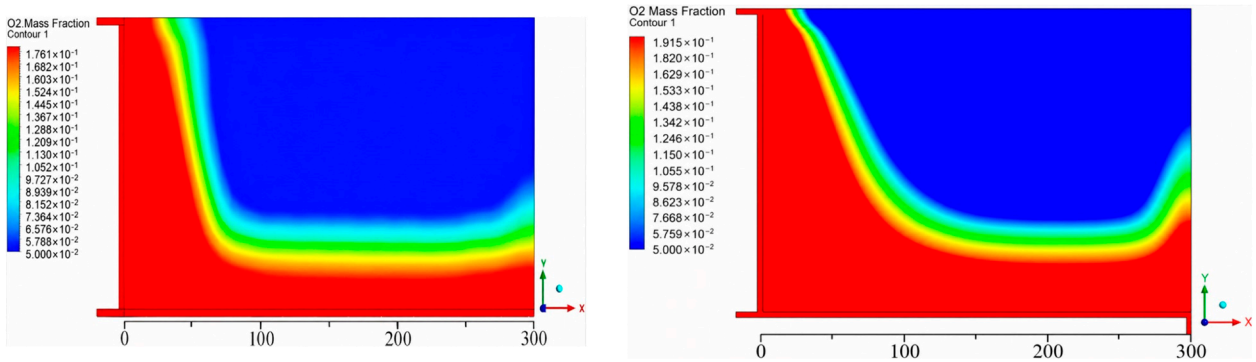
Figure 7. Distribution of velocity streamlines in gob under different ventilation modes.

Under W-type ventilation, the airflow supplied by the 3453S haulage roadway also produces a vortex near the cut-hole corner of the standby face. This occurs because the airflow turns from the standby-face roadway into the gob-side retained entry, creating a deceleration and pressurization zone on the outer side under centrifugal action. The relatively high air-leakage velocity in this region makes it a major leakage pathway. After entering the goaf, part of the airflow migrates inward toward the return airway, whereas the remaining portion returns to the gob-side retained entry. In contrast, Y-type ventilation does not generate an obvious vortex at the tail of the gob-side retained entry. A fraction of the airflow leaks into the goaf through the retained entry, while the rest travels along the working face and is discharged through the return airway.

4.2. Oxygen Concentration and Distribution Characteristics of Spontaneous-Combustion "Three Zones" in Gob Under Different Ventilation Modes

Figure 8 shows that the oxidation zones under both ventilation modes exhibit an L-shaped distribution. Near the working face, oxygen concentration decreases continuously with increasing distance because airflow momentum is progressively dissipated by the obstruction of broken coal and rock. Deeper in the goaf, the compaction degree of the caved material increases, whereas porosity and permeability decrease. Consequently,

airflow resistance becomes higher, air-leakage velocity decreases markedly, and oxygen concentration attenuates more rapidly.



(**a**) Y-type ventilation (**b**) W-type ventilation

Figure 8. Spatial distribution of oxygen concentration in the goaf under different ventilation modes.

Moreover, the continuous open space of the gob-side retained entry tends to maintain persistent leakage channels between the roadway and the goaf. As a result, severe air leakage occurs along the retained-entry side, where a distinct band-shaped oxidation zone develops and remains during face advance.

Comparison of the two ventilation modes reveals that W-type ventilation produces a higher pressure at the tail of the retained entry than Y-type ventilation, thereby enlarging the spontaneous-combustion hazard zone near the cut-hole area. As indicated by Figure 8 and Table 4, the oxidation-zone widths on the retained-entry side are 60 m and 79 m under Y-type and W-type ventilation, respectively. In the W-type layout, the 3453S haulage roadway functions as an intake airway, and part of the supplied airflow directly enters the initial cut-hole area near the working face. The resulting pressure increase not only widens the oxidation zone but also pushes it farther into the goaf.

Table 4. Division of spontaneous-combustion "three zones" in gob with gob-side entry retaining under different ventilation modes.

Ventilation Mode	Location	Oxidation Zone/m	Width of Oxidation Zone/m
Y-type ventilation	Air return roadway	21–68	47
	Retained entry side	22–82	60
W-type ventilation	Air return roadway side	10–29	19
	Retained entry side	37–116	79

CFD-POST post-processing shows that the oxidation zone accounts for 22.5% of the goaf area under Y-type ventilation, which is higher than the 18.3% obtained under W-type ventilation. The observed difference mainly arises from the vortex formation at the end of the gob-side retained entry in the W-type ventilation layout. The vortex drives part of the leaked airflow back toward the working face, thereby reducing the effective air volume that penetrates into the deep goaf. Accordingly, residual coal under Y-type ventilation is exposed to a higher spontaneous-combustion risk.

The comparison between the two ventilation layouts indicates that the spontaneous-combustion risk should be evaluated from both local and overall perspectives. Locally, W-type ventilation produces a higher pressure near the tail of the gob-side retained entry, which enlarges the oxidation-zone width on the retained-entry side from 60 m under Y-type ventilation to 79 m under W-type ventilation. This suggests that W-type ventilation may induce a higher local oxidation risk near the retained-entry side and cut-hole region.

However, from the perspective of the entire goaf, the oxidation zone accounts for 22.5% of the goaf area under Y-type ventilation, compared with 18.3% under W-type ventilation. This difference is mainly attributed to the vortex formed at the end of the gob-side retained entry under W-type ventilation, which drives part of the leaked airflow back toward the working face and reduces the effective air volume penetrating into the deep goaf. Therefore, although W-type ventilation presents a higher local risk along the retained-entry side, Y-type ventilation results in a larger overall oxidation-zone area and thus a higher overall spontaneous-combustion risk within the goaf.

5. Optimization Research on Prevention and Control Technologies for Gob Areas in Gob-Side Entry Retaining

5.1. Study on Air-Leakage Blocking Technology for Fire Prevention and Extinguishing

5.1.1. Field Implementation of Air-Leakage Sealing Measures

Because the caving zone is connected with the gob-side retained entry, the ventilation pressure difference drives airflow from the retained roadway into the goaf, increasing the oxidation risk of residual coal. To reduce leakage, cement blankets were laid on the coal wall of the retained entry, and a small amount of polymer material was sprayed at the interface between the blankets and the roadway to enhance sealing. The cement blanket thickness was 15 mm, and the polymer spray layer was controlled within 50–130 mm. During construction, special grouting equipment was used to mix polymer components A and B uniformly at a mass ratio of 1:1 before spraying, ensuring stable spraying velocity and material dosage. The field spraying process is shown in Figure 9.

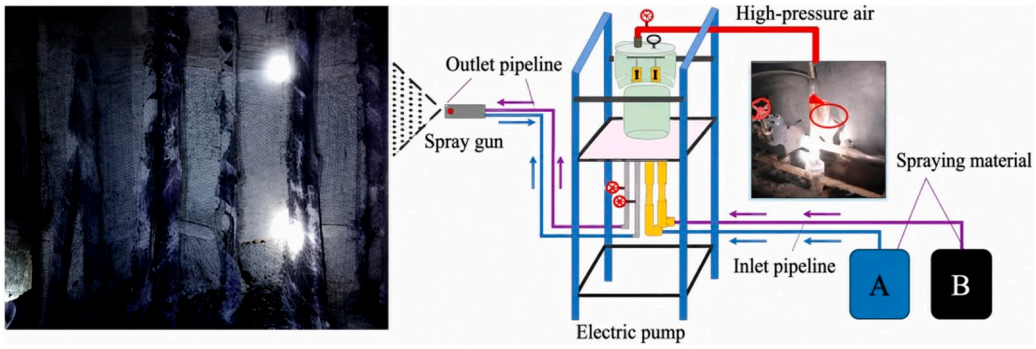


Figure 9. Flow chart of on-site spraying construction. Red arrows and pipelines indicate the high-pressure air supply, blue arrows indicate the inlet pipeline flow direction, and purple arrows indicate the outlet/material delivery pipeline. Containers A and B represent the two polymer components.

5.1.2. Numerical Evaluation of the Air-Leakage Sealing Effect

To evaluate the sealing effect of the gob-side retained entry, the boundary conditions of the model described in Section 3.3 were modified. The interface between the goaf and the gob-side retained entry within 20–300 m was changed from an interior boundary to a porous-jump boundary. Because the leakage-prevention efficiency of the sprayed coating is approximately 90%, the air-passage ratio was set to 10%. The porous-jump boundary was adopted to represent the additional flow resistance introduced by the cement blanket and polymer-spraying coating. These sealing materials form a thin, low-permeability layer along the retained-entry side, which mainly reduces leakage by increasing the pressure loss across the goaf–roadway interface rather than by occupying a large computational volume. Therefore, the porous-jump condition provides a simplified but physically consistent way to describe the resistance effect of the sealing layer without explicitly resolving its small thickness in the numerical mesh. The coating thickness was defined as 0.1 m, while all other boundary conditions were kept identical to those of the original model.

The simulation results in Figure 10 demonstrate that wall spraying and leakage sealing along the gob-side retained entry markedly reduce the heat-dissipation and oxidation zones in the goaf, and the overall spatial distribution of the heat-dissipation and oxidation zones shifts toward the working face. After sealing, the oxidation zone begins 25 m from the working face, and its maximum width decreases to 30 m. On the retained-entry side, the oxidation-zone width is reduced from 60 m to 35 m. These changes indicate that the proposed sealing measure effectively restricts oxygen migration into the deep goaf.

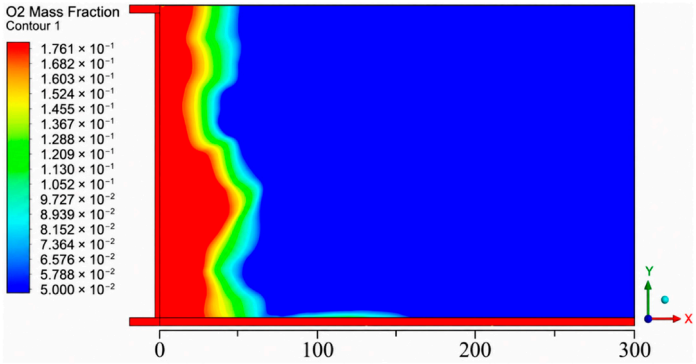


Figure 10. Oxygen concentration distribution in the goaf after spraying and plugging measures along the gob-side retained entry.

5.2. Study on Optimization of Nitrogen-Injection Fire Prevention and Extinguishing Technology

According to the spontaneous-combustion three-zone distribution analyzed in Section 3.2, the oxidation zone under Y-type ventilation extends from 22 m to 65 m on the return-airway side and from 21 m to 55 m on the gob-side retained-entry side. Based on this distribution, a targeted precise nitrogen-injection layout was designed. Nitrogen-injection pipelines were arranged along the strike of the retained entry at equal intervals of 50 m, and each pipeline was designed to extend 30 m into the goaf at the injection position. The pipeline layout is shown in Figure 11.

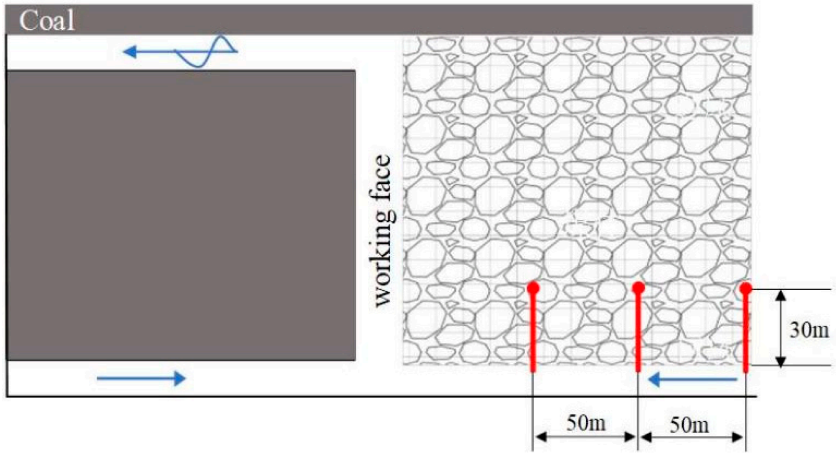


Figure 11. Schematic layout of nitrogen-injection pipelines. Blue arrows indicate airflow direction, red vertical lines represent nitrogen injection pipelines, and the irregular polygonal pattern denotes the caved gangue in the goaf. The grey block represents the working-face/coal-side region.

5.2.1. Parameter Design of Nitrogen Injection for Fire Prevention and Extinguishing in the Working Face

According to Clause 4.3 of the Code for Fire Prevention Design of Coal Mines (GB 51078-2015), the purity of nitrogen used for goaf fire prevention should not be lower than

97%. In addition, the oxygen concentration should be controlled below 7% in conventional inerting zones and below 3% in fire-extinguishing inerting zones. The nitrogen-injection rate for the working face was calculated using the following equation [24,25]:

$$Q_N = 60Q_0 \frac{C_1 - C_2}{C_N + C_2 - 1} \quad (2)$$

where

Q_N—Nitrogen-injection flow rate, m^3/h.
Q_0—Air-leakage quantity, selected as 8 m^3/min.
C_1—Oxygen concentration within the oxidation zone of the goaf without nitrogen injection, generally ranging from 10% to 15%, and taken as 11% in this design.
C_2—The oxygen concentration index for fire prevention inerting in the gob is specified as 7% in accordance with safety regulations.
C_N—Purity of injected nitrogen. In this design, nitrogen produced by a nitrogen generator is adopted with a purity of 97%.

$$Q_N = 60Q_0 \frac{C_1 - C_2}{C_N + C_2 - 1} = 60 \times 8 \times \frac{11\% - 7\%}{97\% + 7\% - 1} = 480 \quad (3)$$

Based on the calculated nitrogen demand, reported engineering experience in goaf nitrogen injection, and the actual mining conditions of the working face, a safety coefficient of 1.2 was adopted. The required capacity of the on-site nitrogen generation system was therefore determined to be greater than 576 m^3/h, satisfying the technical requirements for underground nitrogen-injection fire prevention and extinguishing.

5.2.2. Distribution Characteristics of Spontaneous-Combustion "Three Zones" in Gob Under Different Nitrogen-Injection Flow Rates

Using 600 m^3/h as the baseline nitrogen-injection rate, three additional rates, namely 400, 800, and 1000 m^3/h, were selected for comparative simulation. The corresponding oxygen concentration fields are shown in Figure 12.

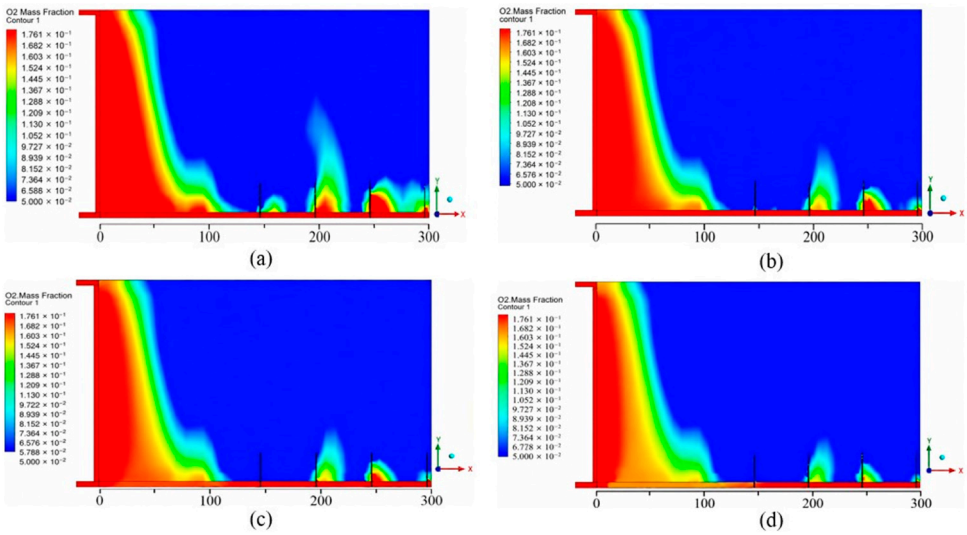


Figure 12. Oxygen concentration distribution in the gob under different nitrogen-injection rates. (**a**)—400 m^3/h; (**b**)—600 m^3/h; (**c**)—800 m^3/h; (**d**)—1000 m^3/h.

Figure 12 shows that, for a fixed nitrogen-injection location, the goaf oxidation-zone area decreases overall as the nitrogen-injection rate increases. At 400 m^3/h, the oxidation zone is markedly reduced, but a limited amount of oxygen still migrates toward the deep goaf under the influence of air leakage. When the injection rate increases to 600 m^3/h,

the higher nitrogen supply raises the internal pressure of the goaf, suppresses air-leakage penetration, and further contracts the oxidation zone.

However, when the nitrogen-injection rate exceeds 600 m^3/h, excessive nitrogen is transported toward the gob-side retained entry by the airflow. This causes the oxygen concentration in some local areas of the retained entry to fall below 20%, leading to abnormal gas distribution. Considering both inerting efficiency and flow-field disturbance, the optimal nitrogen-injection rate under Y-type ventilation is determined as 600 m^3/h. As shown in Figure 13, this rate reduces the oxidation-zone area by 11,160 m^2 compared with the non-injection condition.

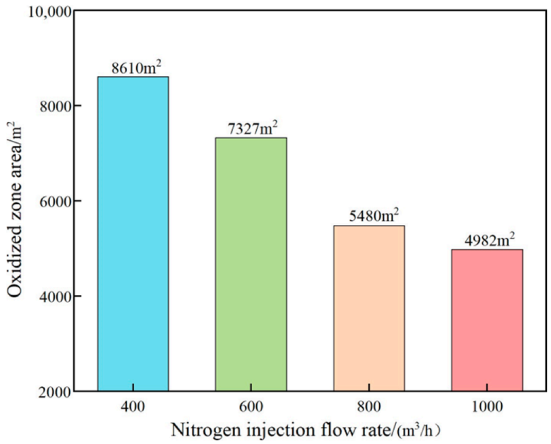


Figure 13. Area of oxidation zone in the gob under different nitrogen-injection flow rates.

6. Field Engineering Validation

To clarify the correspondence between the numerical optimization and field implementation, the prevention and control scheme applied on site was designed according to the optimized parameters obtained in Section 5. The same air-leakage control strategy, including cement-blanket laying and polymer-spraying sealing along the gob-side retained entry, was implemented in the field. In addition, the nitrogen-injection system was operated at the optimized injection rate of 600 m^3/h, which was identified in the numerical simulation as the most suitable value for reducing the oxidation-zone area while avoiding excessive disturbance of the airflow field. The field monitoring of air leakage and CO concentration was therefore used to evaluate the practical performance of the optimized integrated control strategy.

6.1. Field Evaluation of Air-Leakage Sealing Performance

To assess the field performance of the optimized leakage-sealing technology, air-volume measurements were conducted before and after sealing along the gob-side retained entry. Identical monitoring locations were used in both stages to ensure data comparability, and the monitoring layout is shown in Figure 14. A segmented measurement method was adopted within a 250 m section of the retained entry, with monitoring points spaced at 50 m intervals. Six monitoring points were established in total, and the measured air volumes at each point and the leakage volumes between adjacent points are summarized in Table 5.

As shown in Table 5, the measured airflow rate at each monitoring point increased after sealing, indicating improved airflow retention in the gob-side retained entry. However, the airflow increment between adjacent monitoring points became smaller. Based on the cumulative adjacent-point airflow difference, the total leakage volume in the monitored section decreased from 91 m^3/min to 29 m^3/min, corresponding to a reduction of approximately 62 m^3/min.

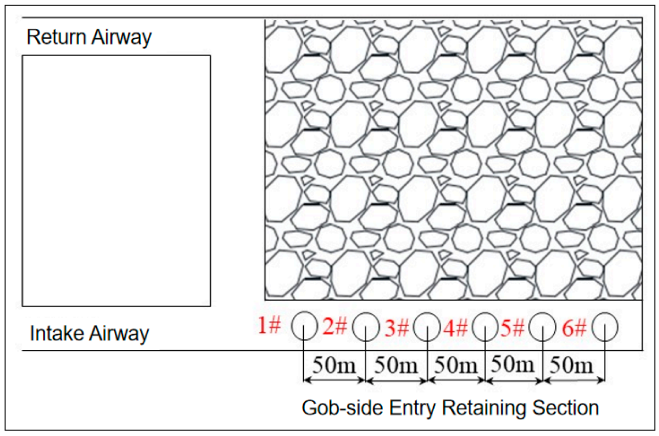


Figure 14. Schematic diagram of on-site air measurement locations. Labels 1#–6# and the corresponding circles denote six airflow-monitoring points arranged along the gob-side retained entry. The black dimension lines indicate that adjacent monitoring points were spaced at 50 m intervals within a 250 m retained-entry section.

Table 5. Measured air volume at each monitoring point.

Measuring Point ID	1	2	3	4	5	6
Air quantity before plugging/$m^3 \cdot min^{-1}$	198	213	229	247	275	289
Air quantity after plugging/$m^3 \cdot min^{-1}$	260	268	272	275	280	289

6.2. Analysis of On-Site Comprehensive Control Effect

After implementation of the proposed residual-coal spontaneous-combustion control technology, continuous monitoring was performed for one month in the area behind the working-face support adjacent to the gob-side retained entry. The control effect was evaluated by analyzing the temporal variation in carbon monoxide (CO) concentration, as shown in Figure 15.

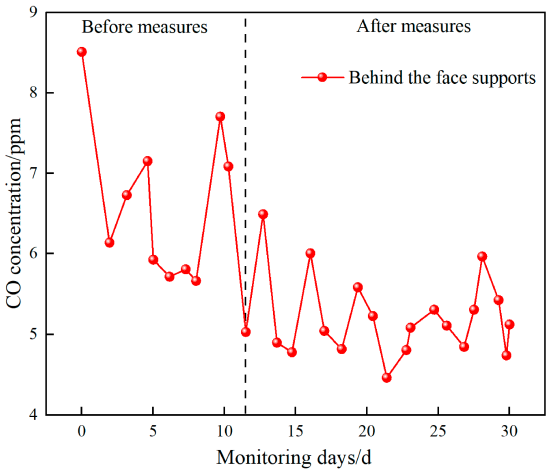


Figure 15. CO concentration variation at monitoring points.

The field monitoring results show that the CO concentration behind the working-face supports adjacent to the gob-side retained entry fluctuates between 4.6 and 8.8 ppm and generally decreases with monitoring time. After application of the proposed control measures, the average CO concentration at the monitoring points remained stable at approximately 4.9 ppm, which is lower than the 24 ppm threshold for CO concentration in

underground mine air. These results provide field evidence for the improved effectiveness of the spontaneous-combustion prevention and control measures.

7. Conclusions

The spatial distribution of the spontaneous-combustion three zones in the gob-side entry retaining goaf was identified by integrating field beam-tube monitoring with Fluent simulation. The oxidation zone exhibited an inclined and continuous band-like morphology, and the close consistency between measured and simulated oxygen concentrations confirmed the reliability of the numerical model. The ventilation layout and air-volume allocation were found to govern the air leakage and oxygen transport within the goaf. Compared with the W-type layout, Y-type ventilation induced a higher spontaneous-combustion risk. Optimizing the air-volume ratio between the 3451S haulage roadway and the gob-side retained entry to 3:1 reduced the oxidation-zone area by approximately 11%, effectively narrowing the hazardous region.

The integrated control strategy combining cement-blanket/polymer-spraying sealing with precise nitrogen-injection effectively suppressed air leakage and limited oxygen diffusion along the gob-side retained entry. At a nitrogen-injection rate of 600 m^3/h, the oxidation-zone area decreased by 11,160 m^2, while the field CO concentration stabilized at approximately 4.9 ppm, providing field evidence for improved fire-prevention performance in the goaf.

Author Contributions: Conceptualization, J.Z. (Jiuling Zhang); methodology, J.Z. (Jiuling Zhang); supervision, J.Z. (Jiuling Zhang); validation, J.F.; formal analysis, J.Z. (Jinghan Zhang); investigation, J.Z. (Jinghan Zhang); resources, R.Z.; data curation, Y.L.; writing—original draft, J.Z. (Jinghan Zhang); writing—review and editing, J.Z. (Jinghan Zhang); visualization, J.Z. (Jinghan Zhang) and Y.L.; supervision, H.N. and R.Z. All authors have read and agreed to the published version of the manuscript.

Funding: This research received no external funding.

Institutional Review Board Statement: Not applicable.

Informed Consent Statement: Not applicable.

Data Availability Statement: The raw data supporting the conclusions of this article will be made available by the authors on request.

Conflicts of Interest: Ruijiang Zhang was employed by Kailuan (Group) Co., Ltd. The remaining authors declare that the research was conducted in the absence of any commercial or financial relationships that could be construed as a potential conflict of interest.

References

1. Hallman, D.S. A review of coal mine fire extinguishment methods. *Emerg. Manag. Sci. Technol.* **2024**, *4*, e005. [CrossRef]
2. Matsobane, E.T.; Onifade, M.; Genc, B.; Bada, S. Comparative investigation of spontaneous combustion of biomass, hydrochar, coal and their blends using Wits-Ehac and thermogravimetric analysis. *Int. J. Coal Prep. Util.* **2024**, *44*, 2155–2179. [CrossRef]
3. Laryea, A.E.N.; Wanxing, R.; Qing, G.; Zenghui, K. Spontaneous coal combustion, direct and indirect impact on mining in China: A prospective review and proposal of a five-level comprehensive mine safety management structure (5L-CMSMS) coupled with hazard zoning and barrier systems. *Combust. Sci. Technol.* **2025**, *197*, 2247–2279.
4. Liang, Y.; Zhang, J.; Wang, L.; Luo, H.; Ren, T. Forecasting spontaneous combustion of coal in underground coal mines by index gases: A review. *J. Loss Prev. Process Ind.* **2019**, *57*, 208–222. [CrossRef]
5. Tang, Z.; Yang, S.; Wu, G. Occurrence mechanism and risk assessment of dynamic of coal and rock disasters in the low-temperature oxidation process of a coal-bed methane reservoir. *Energy Fuels* **2017**, *31*, 3602–3609.
6. Luan, H.; Jiang, Y.; Lin, H.; Li, G. Development of a new gob-side entry-retaining approach and its application. *Sustainability* **2018**, *10*, 470.
7. Fu, J.; Chen, D.; Li, X.; Li, H.; Liu, S.; Li, C.; Zhang, J. Research on the technology of gob-side entry retaining by pouring support beside the roadway in "three soft" coal seam: A case study. *Phys. Fluids* **2024**, *36*, 017123. [CrossRef]

8. Liu, H.; Zhang, B.; Li, X.; Liu, C.; Wang, C.; Wang, F.; Chen, D. Research on roof damage mechanism and control technology of gob-side entry retaining under close distance gob. *Eng. Fail. Anal.* **2022**, *138*, 106331. [CrossRef]
9. Yang, H.; Wang, D.; Ju, W.; Yuan, W.; Su, C. Asymmetric damage mechanisms and prevention technology in Large-Section Gob-Side entry retaining. *Sustainability* **2022**, *15*, 739.
10. Hu, D.; Li, Z. Dynamic distribution and prevention of spontaneous combustion of coal in gob-side entry retaining goaf. *PLoS ONE* **2022**, *17*, e0267631. [CrossRef] [PubMed]
11. Anghelescu, L.; Diaconu, B.M. Advances in detection and monitoring of coal spontaneous combustion: Techniques, challenges, and future directions. *Fire* **2024**, *7*, 354. [CrossRef]
12. Kong, B.; Li, Z.; Yang, Y.; Liu, Z.; Yan, D. A review on the mechanism, risk evaluation, and prevention of coal spontaneous combustion in China. *Environ. Sci. Pollut. Res.* **2017**, *24*, 23453–23470. [CrossRef]
13. Onifade, M. Countermeasures against coal spontaneous combustion: A review. *Int. J. Coal Prep. Util.* **2022**, *42*, 2953–2975.
14. Wu, X.; Dong, J.; Hu, R.; Pang, B.; Si, G. CFD modelling of prevention and mitigation of coal spontaneous combustion in longwall goaf-a comprehensive review and future outlook. *Arch. Comput. Methods Eng.* **2026**, *33*, 3789–3835.
15. Salami, O.B.; Brune, J.F.; Xu, G. A CFD analysis of equipment fires in an underground development heading for improved auxiliary ventilation design. *Saf. Extrem. Environ.* **2025**, *7*, 6. [CrossRef] [PubMed]
16. Zhang, Z.; Chen, X.; Yu, Z.; Sun, H.; Huang, D.; Wu, J.; Zhang, H. Mitigating coal spontaneous combustion risk within goaf of gob-side entry retaining by roof cutting: Investigation of air leakage characteristics and effective plugging techniques. *Fire* **2024**, *7*, 98. [CrossRef]
17. Zhou, X.; Jing, Z.; Li, Y. Research on controlling gas overrun in a working face based on gob-side entry retaining by utilizing ventilation type "Y". *Sci. Rep.* **2023**, *13*, 9199. [CrossRef] [PubMed]
18. Zhou, X.; Jing, Z.; Li, Y.; Bai, G. Study on nitrogen injection fire prevention and extinguishing technology in spontaneous combustion gob based on gob-side entry retaining. *ACS Omega* **2023**, *8*, 30569–30577. [CrossRef] [PubMed]
19. Jing, Z.; Zhou, X.; Li, Y.; Bai, G.; Zhang, S. Research on the technology of uniformly injecting nitrogen into the porous long pipes in the gob of the gob-side entry retaining mining mode with roof cutting and pressure relief. *Sci. Rep.* **2024**, *14*, 18205. [CrossRef] [PubMed]
20. Zhang, J.; Wang, W.; Li, Y.; Li, H.; Zhang, G.; Wu, Y. Fracture distribution characteristics in goaf and prevention and control of spontaneous combustion of remained coal under the influence of gob-side entry retaining roadway. *Energies* **2022**, *15*, 4778. [CrossRef]
21. Luo, X.; Chen, L.; Wu, B.; Sun, M.; Yang, T.; Yu, H. Air leakage characteristics and comprehensive prevention of goaf side retained roadway of fully mechanized mining faces in Qincheng coal mine. *Sci. Rep.* **2025**, *15*, 26342. [CrossRef] [PubMed]
22. Zhao, X.; Dai, G.; Qin, R.; Zhou, L.; Li, J.; Li, J. Spontaneous combustion characteristics of coal based on the oxygen consumption rate integral. *Energy* **2024**, *288*, 129626.
23. Zhang, X.; Wan, Y.; Lu, B.; Huang, G.; Liang, H.; Li, C.; Yu, C. Experimental Study on the effect of Ultraviolet Light on Spontaneous Combustion of coal under the Action of a Photosensitive Reagent. *ACS Omega* **2025**, *10*, 10071–10080. [CrossRef] [PubMed]
24. Qi, Y.; Wang, W.; Qi, Q.; Ning, Z.; Yao, Y. Distribution of spontaneous combustion three zones and optimization of nitrogen injection location in the goaf of a fully mechanized top coal caving face. *PLoS ONE* **2021**, *16*, e0256911. [CrossRef] [PubMed]
25. Wang, W.; Qi, Y.; Liu, J. Study on multi field coupling numerical simulation of nitrogen injection in goaf and fire-fighting technology. *Sci. Rep.* **2022**, *12*, 17399. [CrossRef] [PubMed]

Disclaimer/Publisher's Note: The statements, opinions and data contained in all publications are solely those of the individual author(s) and contributor(s) and not of MDPI and/or the editor(s). MDPI and/or the editor(s) disclaim responsibility for any injury to people or property resulting from any ideas, methods, instructions or products referred to in the content.